EFDA–JET–PR(08)15

O. Asunta, T. Kurki-Suonio, T. Tala, S. Sipilä, R. Salomaa,
and JET-EFDA contributors

Comparison of Fusion Alpha Performance in JET Advanced Scenario and H-mode Plasmas

Comparison of Fusion Alpha Performance in JET Advanced Scenario and H-mode Plasmas

O. Asunta[1], T. Kurki-Suonio[1], T. Tala[2], S. Sipilä[1], R. Salomaa[1], and JET EFDA contributors*

JET-EFDA, Culham Science Centre, OX14 3DB, Abingdon, UK

[1]Helsinki University of Technology, Association Euratom Tekes, PO Box 4100, 02015 TKK, Finland
[2]Association Euratom Tekes, VTT, P.O.Box 1000, FI-02044 VTT, Finland
** See annex of M.L. Watkins et al, "Overview of JET Results ", (Proc. 21st IAEA Fusion Energy Conference, Chengdu, China (2006)).*

Preprint of Paper to be submitted for publication in
Plasma Physics and Controlled Fusion

ABSTRACT.

Optimizing the energy production in a fusion reactor requires a broad hot and dense region in the plasma core. The edge, however, should be cool in order to maintain the integrity of the first wall. In this work the confinement and heating profile of fusion alphas were studied in realistic JET geometry. The magnetic fields, as well as temperature and density profiles from four JET discharges, including two ELMy H – mode plasmas and two ITB plasmas with reversed q-profiles, were used as backgrounds for the simulations. The work was carried out using the Monte Carlo – based guiding-center-following code ASCOT.

For the same plasma current, the ITB discharges were found to produce three to seven times more fusion power than the comparable ELMy H – mode discharge. Unfortunately, also the alpha particle losses were larger (10 –16%) compared to the H-mode discharge (6%). In the H-mode discharges, alpha power was deposited to the plasma symmetrically around the magnetic axis, whereas in the current hole discharge, the power was spread out to a larger volume in the plasma center. This was due to larger particle orbits, and the larger spacing of the innermost flux surfaces.

1. INTRODUCTION

The main goal of a fusion reactor is to produce energy. Since the fusion reaction rate and, thus, the energy production are strongly dependent on ion temperature and density, optimizing these quantities is essential when designing a fusion reactor. However, if the plasma is hot close to the separatrix, lot of fast particles will escape from the plasma, causing a threat to the integrity of the first wall. Therefore, the ideal plasma profiles would have a wide hot and dense region around the plasma core, and a cool edge.

One way to maintain this kind of pro les is by creating a so – called Internal Transport Barrier (ITB) [1]. An ITB is observable in Fig. 1a presenting the temperature and density profiles of a JET discharge #51976; the ion temperature is very high in the plasma core and low at the edge. However, achieving this kind of profiles comes at a price. Traditionally, ITBs are observed in advanced scenario plasmas, characterized by a reversed magnetic shear in the plasma center. For brevity we shall refer to such a profile simply as reversed as opposed to normal monotonic q – profile. Reversed q-profile can be created by a low or vanishing toroidal current in the plasma center, which decreases the poloidal magnetic field and, consequently, increases the widths of fast particle orbits.

In this work the con nement and heating pro le of fusion alphas were studied in realistic JET geometry. Two standard JET ELMy H-mode plasmas (discharges #50844 and #52009) with a monotonic q – profile, as well as two ITB plasmas (discharges #51976 and #66498) with a reversed q-profile were used as backgrounds for the simulations. The discharge #51976 was particularly interesting since it exhibited a current hole. To work out the effect of the q-profile on the confinement of alpha particles, a discharge with a similar total fusion rate, but a monotonous q-profile (#52009) was needed. Due to the importance of the poloidal magnetic eld in con ning the plasma, it was also

of interest to study an H – mode discharge (#50844) with the same plasma current as the current hole discharge #51976. Discharge #66498 was also studied in order to have one discharge with a reversed q-profile, but without a current hole.

The work was carried out using the Monte Carlo - based guiding-center-following code ASCOT [2]. The effect of the q-pro le to the alpha particle behavior has been studied earlier with ASCOT in a circular symmetry with analytic plasma profiles [3], but in this work it was done in realistic JET geometry with experimental temperature and density pro les. This work also complements the earlier Fokker – Planck analysis [4] not only by using a completely different method but also by allowing the experimental flux surface structure which, in the center of an ITB plasma, does not easily render itself to simple parametrization.

The structure of the paper is as follows. In Sec. 2 the orbits of fusion – born alpha particles are discussed. Section 3 briefly describes ASCOT and outlines the course of the simulations performed in this work. The simulated discharges are introduced in more detail in Sec. 4. Section 4 also presents the results of the simulations; the losses and power deposition of the alpha particles. Conclusions are drawn and discussed in Sec. 5.

2. ORBITS OF FUSION-BORN ALPHA PARTICLES

The motion of a charged particle in an electromagnetic eld is described by the equation

$$\frac{\mathrm{d}}{\mathrm{d}t}\, m\mathrm{V} = \mathrm{Z}e(\mathrm{E} + \mathrm{v} \times \mathrm{B}), \tag{1}$$

where m is the mass, Z is the charge number and v is the velocity of the particle, E and B are the electric and the magnetic field, respectively, and e is the elementary charge. It is a computationally demanding task to simulate the exact motion of a particle accurately and, therefore, it is often approximated by the motion of the particle's guiding-center. For the guiding – center approximation to be valid, the electric and magnetic fields as well as background temperatures and densities experienced by the particle over a single Larmor orbit should be almost constants. For the magnetic field,

$$r_L \left|\frac{\nabla B}{B}\right| \sim \frac{\upsilon_\perp}{\Omega} \left|\frac{\nabla B}{B}\right| \ll 1, \tag{2}$$

where $r_L = \upsilon_\perp/\Omega = mv_\perp/ZeB$. It should be born in mind that, in reality, the particle can be quite far from its guiding-center. For example in JET, in a magnetic field of 2.5T, a typical fusion-born 3.5 MeV alpha particle, that has its energy evenly divided between parallel and perpendicular velocities, has a Larmor radius of 7.6cm. Using the guiding – center approximation, the electric and magnetic elds as well as the plasma parameters are evaluated only at the location of the guiding-center and, thus, all the effects stemming from particle's finite Larmor radius are lost.

Averaging Eq. (1) over the gyromotion of the particle we get the guiding-centerequation of motion,

$$v_{gc} = \frac{v_{\|}B}{B} + \frac{1}{2\Omega}\frac{v^2 + v_{\|}^2}{B^2}(B \times \nabla B) + \frac{E \times B}{B^2} \quad (3)$$

The first term of the equation represents the motion of the particle along the field line, and the two latter ones stand for drifts. The second term in Eq. (3), henceforth called the gradient drift, represents the drifts due to the gradient and the curvature of the magnetic field. Because the gradient of the magnetic field always points toward the center of the torus, and the magnetic field points predominantly to the toroidal direction, the B x ∇B – term tends to drift the particles up or down, depending on the direction of the magnetic eld and the charge of the particle. The third term in Eq. (3) is due to the electric field.

For studying the particle trajectories in the poloidal cross-section of a device, it is practical to write out the z-component of the guiding-center equation of motion, Eq. (3). This is because the gradient drift, pointing down in the discharges studied in this work, is the dominant drift. Using only highest order terms one gets

$$\frac{dz}{dt} = v_{\|}\frac{B_\theta}{B_{tot}}\frac{x}{r} - \frac{m}{2ZeB_{tot}}\frac{v^2 + v_{\|}^2}{B_{tot}^2}\frac{B_0^2 R_0^2}{(R_0 + x)^3}, \quad (4)$$

where the center of the cartesian (x; z) – coordinate system is at the magnetic axis. In Eq. (4), the E x B-drift has been omitted since, apart from the edge of the plasma, it is small compared to the gradient drift. From now on, we consider only the outer equatorial plane, since all the particles born on the LFS of the device must cross it at some point during their orbit. Near the outer equatorial plane, r ≈ x. Assuming, in addition, a large aspect ratio, $R_0 + x \approx R_0$, and that $B_{tot} \approx B_\phi \approx B_\theta$, Eq. (4) becomes

$$\frac{dz}{dt} = v_{\|}\frac{B_\theta}{B_{tot}} - \frac{m}{2Ze}\frac{(v^2 + v_{\|}^2)}{R_0 B_{tot}} \quad (5)$$

The assumption of a large aspect ratio is quite rough and it is done only in order to simplify the equation for qualitative examination of the drift orbit topologies.

In a tokamak, particle orbits can be crudely divided into two categories: untrapped and trapped orbits. The former group consists of orbits that encircle the magnetic axis, while circling the tokamak always in the same toroidal direction. The latter group, on the other hand, consists of all the orbits that do not encircle the magnetic axis and are, thus, trapped on one side of the device. The classi cation of the orbits can be done in a much more detailed fashion. For example Eriksson and Porcelli [5] divide guiding - center orbits into nine characteristic groups. For this work, however, it suffices to distinguish three drift orbit topologies: passing, banana, and potato orbits. Here the first one is an untrapped orbit, whereas the latter two are trapped. Because the first two are well-known standard orbits, they will not be further discussed. Instead, emphasis is put on describing the birth of potato orbits because of their importance for high-energy particles.

Unlike in the case of passing and banana orbits, a unique definition for potato orbits does not

exist in the literature. However, according to all the definitions potatoes can be thought of as banana orbits, distorted by the gradient drift. If the gradient drift is not quite strong enough to pull the particle across the midplane before it reaches its turning point, the result is a wide, rotund banana orbit, possibly enclosing the magnetic axis. Some authors would, nevertheless, recognize it as a potato orbit, since sometimes potato orbits are understood as a subclass of banana orbits, which either enclose the magnetic axis [6], or are so wide that their widths are comparable to their radial positions [7].

In this work, however, an orbit will be called a potato only if the gradient drift is strong enough to pull the particle across the midplane before it reaches the magnetic axis or its turning point, thus making the orbit poloidally trapped on one side of the magnetic axis, like a banana orbit, but toroidally untrapped, like a passing orbit. Given this definition, the potato orbits can also be regarded as distorted passing orbits and, thus, they lie somewhere in between the banana and the passing orbits. This definition of potato orbits is adopted from [3]. The vertical motion of a particle is a result of a competition of the two terms in Eq. (5), i.e., the poloidal component of the parallel velocity, and the gradient drift. If the total kinetic energy of a particle is large and the poloidal magnetic field as well as the parallel velocity of the particle are small enough, the gradient drift can dominate the vertical motion.

For example, take a fast alpha particle born on the outer midplane with a positive pitch, $\xi = v_{\|}/v > 0$. If its parallel velocity is sufficiently large, the particle starts moving upward following the field line. However, the particle feels the gradient drift pulling it down and, depending on its initial parallel velocity, the gradient drift may start to dominate as the particle drifts closer to the magnetic axis (i.e. B_θ decreases). This results in the particle moving downwards and, after crossing the midplane, at the same time further away from the magnetic axis. Consequently, the poloidal magnetic field increases and, eventually, the first term in Eq. (5) starts to dominate, yet again moving the particle upward.

Due to their origin, potato orbits exist on both sides of the magnetic axis, unlike banana orbits that only appear on the Low – Field side (LFS) of the device. On the Low – Field side, the pitch of the particle has to be positive for the potato orbits to appear. On the High – Field side (HFS) the directions of the particle velocities are, naturally, reversed.

At the midplane of the device, there can be a point where particles' vertical motion due to following the field line exactly cancels out the B x ∇B drift. This causes the righthand - side of Eq. (5) and, consequently, the vertical motion of the particle, to reduce to zero. Such a point is called the stagnation point [8]. The location of the stagnation point depends on the energy and the pitch of the particle. In theory, if a particle was born at its stagnation point, it would have no vertical velocity and would only be moving in the toroidal direction. In practice, however, all the particles are only born close to the stagnation point and, therefore, have some vertical velocity. Such particles encircle their stagnation point on minuscule stagnation orbits. Actually, the stagnation orbits are just a special case of potato orbits, since also potato orbits encircle their respective stagnation points. The radius of the smallest stagnation orbits is of the order of a few centimeters. As was mentioned

above, the Larmor radii of energetic alpha particles are often larger than that. Therefore, in the case of the smallest stagnation orbits, the Larmor radius actually dominates the particle motion. In ITER, this is not the case, as the magnetic field in ITER is roughly twice the magnetic field in JET and, thus, the Larmor radii of 3.5MeV alpha particles are halved.

3. SIMULATING FUSION ALPHAS WITH ASCOT

ASCOT [9] is a test-particle Monte Carlo code, that traces electron or ion guiding – center orbits in a three – dimensional tokamak geometry. ASCOT follows a limited number of so – called test particles, each representing a group of real particles. Each test particle is given a weight factor to indicate the number of real particles it represents. In this application, for example, the weight factors are assigned according to the local fusion rate [10], i.e the birth rate of the fusion alphas.

A test particle with a random pitch $\xi \in [-1, 1]$ is initialized in each grid cell of an equally spaced rectangular (R, z)-grid within the given lower and upper limits ρ_{min} and ρ_{max}. Here ρ is the normalized poloidal magnetic flux, often used as a radial coordinate. The pitch has a strong effect on the behavior of the particle and, therefore, the entire range $[-1, 1]$ should be covered as uniformly as possible. This is achieved by means of high spatial density of the test particles. For this work, ensembles of about 100 000 test alphas were simulated.

In ASCOT, the particles are followed by numerically integrating their guiding – center equation of motion over time [11]. ASCOT assumes a steady – state plasma background and can take into account the e ects of a toroidal electric eld, Coulomb collisions, and radio-frequency (RF) waves on the particle orbits. However, in this work only the collisions were included. The interactions a ecting the particle's velocity components are evaluated between time steps using Monte Carlo operators. The time step, Δt, is a fraction of the bounce time for trapped particles, and a fraction of the transit time around the magnetic axis for passing particles. In the simulations performed for this work, $\Delta t = \tau_B / 100$ was used in order to reproduce the orbit topologies with sufficient accuracy, yet without excessive use of computing time.

Due to the high energy of the fusion alphas, they lose energy predominantly via collisions with the background electrons. The collisional processes are modeled using binomially distributed Monte Carlo operators derived from the Landau limit of the relativistic Balescu – Lenard collision operator for non-relativistic field particles [12]. The resulting Monte Carlo operator for modeling the effect of Coulomb collisions on the energy of the test particle is given by [13]:

$$\begin{aligned} \Delta\varepsilon &= \Delta\varepsilon_f + \delta_2 \Delta\varepsilon_s \\ &= -\sum_j 2 v_{\varepsilon,j} \Delta t \left[\varepsilon - - \gamma k_B T_j - p_1 \frac{k_B T_j}{2} \frac{d\gamma}{\mathrm{d}p_1} - \frac{1}{2} \frac{\gamma k_B T_j p_1}{v_{\varepsilon,j}} \frac{dv_{\varepsilon,j}}{\mathrm{d}p_1} \right. \\ &\quad \left. + \delta_2 \left[\sum_j 4\gamma k_B T_j \varepsilon v_{\varepsilon,j} \Delta t \right]^{1/2} \right. \end{aligned} \tag{6}$$

where $\nu_{e,j}$ and T_j are the energy collision frequency and the temperature for plasma species j, respectively, k_B is the Boltzmann constant, p is the relativistic momentum of the test particle, γ is the relativistic factor, and δ_2 is the evenly distributed random sign (+1 or −1). The first term on the right-hand side of the equation is the friction term $\Delta\varepsilon_f$, which tends to thermalize the particle. The second term, $\Delta\varepsilon_s$, is the stochastic term producing the standard deviation of the Maxwellian energy distribution. Equation (6) reduces to that of Ref. [14] at non-relativistic energies.

During the simulation, the change in particle energy was recorded, along with its location in the poloidal cross − section, yielding the two − dimensional power deposition profile. All the test particles were simulated from the moment they were born until they either hit a material surface or had only 100keV of their energy left. At such an energy, a fusion-born alpha particle has already lost nearly all (over 97%) of its energy and, thus, the rest is insignificant.

4. ALPHA PARTICLE POWER DEPOSITION IN JET DISCHARGES

4.1. SIMULATED DISCHARGES

In this work the confinement and heating profile of fusion alphas were studied in both standard ELMy H − mode plasmas (JET discharges #50844 and #52009) with a monotonic q−profile, and ITB plasmas (discharges #51976 and #66498) with a reversed q-profile. What makes discharge #51976 special is a current hole, the effect of which is shown in Fig. 2 depicting the flux surface structures of the four discharges. The current hole not only increases the radii of the innermost flux surfaces, but it can also break their concentricity (see Fig. 2a). The flux surfaces of the H − mode discharges #50844 and #52009 are regular and concentric, as are the flux surfaces of the ITB discharge #66498 with a reversed q-profile, but without a current hole. The non − concentricity of the magnetic structure seen in Fig. 2a is not a characteristic feature for current hole discharges. It may not even be real but merely an artifact appearing in calculating the magnetic equilibrium due to the unusually small poloidal field.

Considering the ability of a magnetic field to confine charged particles, the poloidal component of the field, created by the toroidal current, is essential. Therefore, it was also of interest to study an H-mode discharge (#50844) with the same 1.9MA plasma current as the ITB discharges #51976 and #66498. Discharge #52009, on the other hand, had a large 2.5MA plasma current. The plasma currents should be born in mind when comparing the particle confinement in these discharges.

The fusion rates of the studied discharges, plotted in Fig. 3b, were calculated directly from the density and temperature profiles, assuming the plasmas to be 50:50 mixtures of deuterium and tritium, and using the parametrized formulas presented in Ref. [10]. Figure 3 demonstrates how, even though discharges #66498 and #52009 have the highest fusion densities in the plasma core, the total amount of fusion reactions there is largest for the discharge #51976. This is clearly due to the large volumes of the innermost flux surfaces in discharge #51976 (Fig. 2a). It should also be noted how the shape of the plasma profiles affects the fusion rate; for the ITB discharges with steep profiles (recall Fig. 1) the fusion rate distributions are narrower and reach their maxima closer to the plasma core than

the H-mode discharges. Summing up the total fusion rates of the studied discharges shows that the H-mode discharge #52009 has the highest total fusion rate, thanks to its wide temperature and density profiles. However, comparing the rest of the discharges, all with the same plasma current, the total fusion rates in the ITB discharges, #51976 and #66498, are signicantly higher than in the ELMy H – mode discharge #50844. As Fig. 3b illustrates, the fusion rate (i.e. alpha birth rate) profiles of the three shots are very similar from $\rho = 0.5$ outward. This could lead to a conclusion that also the alpha particle losses of the three discharges should be of the same magnitude. As will be seen in the following Section, that is, however, not the case.

4.2. POWER LOSSES

The total power deposited on the walls of the device, i.e. the wall loads, by the alpha particles were substantial in the discharges with a reversed q – profile. In discharge #51976, the total wall load was 11.3kW, which represents 16% of the fusion power carried by the alpha particles. For the discharge #66498 the same gures were 4.1kW and 10%. In the H-mode discharge #50844 with the same plasma current as in the discharges with a reversed q-profile, the wall loads were notably smaller. Only 0.75kW (6%) of the alpha power was deposited to the walls. In discharge #52009 with a larger plasma current, the wall loads were further reduced to 2.9 kW (3%). The fraction of first orbit losses was observed to be slightly over 90% of the total alpha losses in all the discharges.

The confining e ect of the plasma current can be clearly seen from the total losses: in H – mode discharges, increasing the plasma current from 1.9MA to 2.5MA roughly halved the alpha losses. It has been suggested that reduction of losses could also be achieved in the discharges with a reversed q-profile [4]. Unfortunately, the results presented above combined with an earlier study by Schneider et al. [15] do not confirm this. In Ref. [15], they studied alpha particles in JET current hole discharge #61341 using the orbit following Monte Carlo code SPOT [16]. According to them, the total loss of alpha particle power was 15%, of which 90% was due to the first orbit losses. These results are practically identical to our results for the current hole discharge #51976. However, the plasma current in #61341 was 2.8MA compared to only 1.9MA in #51976. Such an increase in plasma current was anticipated to have a substantially larger impact on the alpha losses.

Another study by Yavorskij et al., using three - dimensional predictive Fokker-Planck simulations with a semi-analytical magnetic background, reported alpha power losses of about 35% of the total alpha power for the discharge #51976 [4]. The Fokker-Planck simulations take into account the entire phase space, but their wide scope comes with a price in the form of loss of details. The particle-following codes ASCOT and SPOT, on the other hand, produce "noisy" results due to the nite number of simulated particles, but resolve all the possible orbit topologies accurately. This partly explains the difference in the results between the two types of approaches. Another potential reason for the variation in the results for the JET discharge #51976 is the semi – analytical magnetic background, used in [4], that completely ignores the non-concentric magnetic structure of the discharge (recall Fig. 2a). This naturally has a major impact on the particle orbits and, consequently, on the losses.

Quantitative differences aside, the Fokker – Planck and the particle-following simulations complement each other, and can thus consolidate each other's results. Obtaining qualitatively similar results with these two independent methods improves the reliability of the results.

4.3. POWER DEPOSITION ON THE PLASMA

The power deposition to the plasma as well as the wall loads in the four discharges have been collected in Table 1. The total fusion power carried by the alpha particles, calculated from the plasma profiles, is presented on the bottom line of the table, whereas the second line from the bottom shows the sum of the simulated losses. The difference between the total deposited power and the produced fusion power to alpha particles is mainly due to ending the simulations when particles still had 100keV of their energy left and, to a lesser extent, numerical inaccuracies in the simulations. From Table 1 it seems obvious that discharge #52009 is the most feasible pulse for power generation, since it has a substantial fusion power with minimal losses. It should, however, be born in mind that discharge #52009 has higher plasma current than the rest of the studied discharges. Comparing the discharges with the same plasma current it seems that even though the losses are greater in discharges with a reversed q-profile, also the power generation in them is substantially larger due to their peaked ion temperature profiles. It is also of interest how the deposited power is distributed inside the plasma.

In the H – mode discharges the alpha particles were, not surprisingly, observed to heat a relatively symmetric region around the magnetic axis. Also the effect of the plasma current I_p is evident from the simulations of the two H-mode discharges #50844 (I_p = 1.9MA) and #52009 (I_p = 2.5MA). As had been assumed, e.g. by Yavorskij et al. [4], the larger plasma current in the discharge #52009 and the consequent larger poloidal magnetic field resulted in narrower orbits and better confinement of the alpha particles compared to the discharge #50844. In the discharge #52009 the alphas, mostly born close to the center of the plasma, also stay close to it and, thus, their energy is deposited in a smaller region near the magnetic axis. Also in the plasma with a reversed q – profile, but without a current hole (#66498), the power deposition was narrow and fairly symmetric around the magnetic axis. This was due to highly peaked temperature and density profiles and small spacing of the innermost flux surfaces (recall Fig. 2).

The power deposition pattern for a current hole plasma, depicted in Fig. 4b, is quite different compared to the ones observed in H-mode plasmas, e.g. Fig. 4a. First, even though there are maxima of power deposition located close to both magnetic axes, the structure of the power deposition pattern does not follow the same logic of being hot in the center and clearly cooling outwards. Instead, in addition to the maxima near the two magnetic axes, there are several hot spots and one cooler region, where a more or less even power distribution was expected. Second, the volume heated by alpha particles is much larger in the current hole plasma.

The results of single particle simulations on large scale phenomena such as the plasma heating by power deposition are but a sum of the contributions of individual particles. Therefore, the

characteristic features of the power deposition pattern seen in Fig. 4b can be understood by studying the trajectories of individual alpha particles. The vanishing toroidal current in the plasma core results in a non-existent poloidal magnetic field. Consequently, the particle trajectories in the center of the plasma are dominated by the gradient drift and, thus, are almost vertical. The gradient drift slowly moves the particles downward and they spend a lot of time inside the current hole, relative to the time they spend outside of it. Thus, they also deposit a lot of energy to the plasma inside the current hole. This explains the high power deposition throughout the center of the current hole seen in Fig. 4b. Obviously, the larger the current hole, the larger the heated volume.

When a particle reaches the edge of the current hole, it quickly turns and starts following the magnetic field lines. That is the reason for a large amount of alpha particle orbits having their turning points in the same region in the poloidal plane. This is illustrated in Fig. 5a that depicts orbits of randomly - chosen alpha particles born in the region of the device with the highest amount of fusion reactions per second. Figure 5a also reveals the reason why the plasmas with a reversed q - profile exhibit substantially higher alpha losses, even though their fusion rates in the outer parts of the plasma, $\rho \geq 0.5$, are very similar to H-mode discharge #50844 (recall Fig. 3b): In plasmas with a reversed q-profile, significant part of even the alpha particles born in the middle of the plasma, are lost on their first orbit.

The poloidal velocity of a particle slows down at the tip of its banana or potato orbit. Thus, a particle spends more time close to its turning points than elsewhere. Fig. 5a shows that majority of the particle orbits have their turning points at the same location resulting in maxima in the power deposition. The upper turning point is more evident from the power deposition pattern (two dark red squares in Fig. 4b), but also the lower one can be distinguished. The difference in magnitude between the two turning points arises from the up – down asymmetry of the magnetic flux surface structure. It results in the alpha particles making a sharper turn at the upper turning point, which causes them to spend more time and, consequently, depositing more energy, in a smaller volume.

The birth mechanism of the cool region with a hot spot in the middle, located on the LFS of the device, can also be understood with the help of Figs. 5a and b depicting characteristic alpha particle orbits. As Fig. 5a demonstrates, majority of the alpha particle orbits encircle a small region of the plasma. Since hardly any alphas enter this region, it receives very little heating. There is, however, one hot spot inside the cold region caused by the stagnation orbits. The stagnation orbits were discussed in Sec. 2 and are visible in Fig. 5b as a solid green circle. Some alphas born close to the stagnation point also remain close to it and end up depositing all their energy in an extremely small volume. Even if the number of particles behaving this way is relatively small, having all their energies deposited in a small volume is enough to cause a maximum in the power deposition profile. As the detailed view of the plasma center presented in Fig. 6 illustrates, a similar structure is found also on the HFS of the device.

The location of the stagnation point matches well with the findings of Hawkes et al. [17]. They were studying experimentally the distribution of fast tritium ions in JET current hole plasmas

and were able to locate a stagnation point at approximately 0.2m from the magnetic axis. A more enlarged view of the fine structure of the power deposition pattern, presented in Fig. 6, shows that, also in the simulations, the distance of the stagnation point from the magnetic axis is, indeed, about 0.2m.

5. CONCLUSIONS AND DISCUSSION

The power deposition and losses of 3.5 MeV fusion-born alpha particles were studied by following the alpha particle orbits with the guiding-center-following Monte Carlo code ASCOT. The main emphasis was on investigating the performance of the alpha particles in an advanced scenario plasma and comparing it to their behavior in standard ELMy H-mode plasmas. For this purpose a JET advanced scenario discharges #51976 and #66498, along with two H-mode discharges, #50844 and #52009, were used as backgrounds for the simulations.

Compared to H-mode plasmas, the confinement of alpha particles in ITB plasmas was found out to be substantially worse. In discharge #51976 the losses represented approximately 16%, and in discharge #66498 about 10% of the total alpha particle power. For the H-mode discharge #50844 with the same plasma current as the ITB plasmas, the losses were only about 6% of the alpha power. First orbit losses comprised over 90% of all the alpha particle losses in all the discharges, and it is worth noting how, in the plasmas with reversed q-profiles, significant amount of even the particles born in the plasma core experience first orbit losses. Therefore, having a cold edge with very few fusion reactions is not enough to protect the first wall from the fusion alphas. In the H – mode plasmas studied in this work, an increase of the plasma current from 1.9MA to 2.5MA reduced the alpha losses to about one half, i.e. from 6% to 3% of the total alpha power. However, the results presented here and in [15] indicate that increasing the total plasma current in plasmas with a reversed q-profile might not work as well.

As expected, the power deposition in H-mode discharges was observed to be located symmetrically around the magnetic axis. In the more interesting current hole discharge #51976, the power deposition was distributed to a larger volume in the plasma center due to the large spacing of the innermost flux surfaces and wide particle orbits. Also distinct hot spots, caused by stagnation orbits and the tips of potato orbits, were observed in the power deposition pattern. In the ITB discharge without a current hole (#66498), the power deposition was symmetric and even more centered than in the H–mode plasmas.

What comes to the ability of the alpha particles to heat the plasma, it is not obvious which one is better, an ITB or an H – mode plasma. In the ITB plasmas the temperatures in the plasma center are very high and, consequently, they have higher fusion yields than an H-mode plasma with the same plasma current. Thus, even with higher losses, ITB plasmas still deposit more power to the plasma. Power is mainly deposited to the electrons and, thus, in the case of a wide power distribution, such as in #51976, the electrons might diffuse out from the plasma core before transferring their power to the ions. However, this is not problem if the electrons are confined well enough by the ITB.

ACKNOWLEDGEMENTS

This work was carried out as a part of the Association Euratom Tekes activities within the framework of the European Fusion Development Agreement. The views and opinions expressed herein do not necessarily re ect those of the European Commission. The computing facilities of the Finnish IT Center for Science (CSC) used in this work are thankfully acknowledged.

REFERENCES

1. X. Litaudon T. Aniel, Y. Baranov, D. Bartlett, A. Bécoulet, C. Challis, G.D. Conway, G.A. Cottrell, A. Ekedahl, M. Erba, L. Eriksson, et al., Plasma Phys. Control. Fusion 41, A733 (1999).
2. J.A. Heikkinen, T.P. Kiviniemi, T. Kurki-Suonio, A.G. Peeters, and S.K. Sipilä, J. Comp. Phys. 173, 527 (2001).
3. T. Kurki-Suonio, V. Tulkki, S. Sipilä, and R. Salomaa, Plasma Phys. Control. Fusion 48 (9), 1413 (2006).
4. V. Yavorskij, V. Goloborod'ko, K. Schoepf, S.E. Shaparov, C.D. Challis, S. Reznik, and D. Stork, Nucl. Fusion 43, 1077 (2003).
5. L.- G. Eriksson and F. Porcelli, Plasma Phys. Control. Fusion 43, R145 (2001).
6. R.B. White, The Theory of Toroidally Con ned Plasmas (Imperial College Press, London, 2001), 2nd ed.
7. K.C. Shaing, A.Y. Aydemir, Y.R. Lin-Liu, and R.L. Miller, Phys. Rev. Lett. 79, 3652 (1997).
8. J.A. Rome and Y-K.M. Peng, Nucl. Fusion 19 (9), 1193 (1979).
9. J.A. Heikkinen and S.K. Sipilä, Phys. Plasmas 2, 3724 (1995).
10. H.-S. Bosch and G.M. Hale, Nucl. Fusion 32, 611 (1992).
11. J.A. Heikkinen, S.K. Sipilä, and T.J.H. Pättikangas, Comp. Phys. Comm. 76, 215 (1993).
12. I.B. Bernstein and D.C Baxter, Phys. Fluids 24, 108 (1981).
13 S. Sipilä, Monte Carlo Simulation of Charged Particle Orbits in the Presence of Radio frequency Waves in Tokamak Plasmas, Ph.D. thesis, Helsinki University of Technology (1997).
14. A.H. Boozer and G. Kuo-Petravic, Phys. Fluids 24, 851 (1981).
15. M. Schneider, L.-G. Eriksson, V. Basiuk, and F. Imbeaux, Plasma Phys. Control. Fusion 47, 2087 (2005).
16. M. Schneider, L.-G. Eriksson, V. Basiuk, and F. Imbeaux, SPOT: a New Monte Carlo Solver for Fast Alpha Particles (visited 22.8.2006), http://hal.ccsd.cnrs.fr/ccsd-00002037/en/.
17. N.C. Hawkes, V.A. Yavorskij, J.M. Adams, Yu. F. Baranov, L. Bertalot, C.D. Challis, S. Conroy, V. Goloborod'ko, V. Kiptily, S. Popovichev, et al., Plasma Phys. Control. Fusion 47, 1475 (2005).

	#51976	#50844	#52009	#66498
I_p (MA)	1.9	1.9	2.5	1.9
Power losses to the wall	11.3	0.75	2.9	4.1
Power to plasma electrons	52	9.7	79	34
Power to plasma ions	4.8	0.32	3.9	2.7
Total	68.1	10.8	85.8	40.8
Fusion power to alpha particles	69.5	13.6	87.8	42.1

Table 1: Fusion power carried by alpha particles (bottom line), and power deposition to the electrons, ions, and the first wall in kilowatts (kW), for the discharges under consideration. The small di erence between the total deposited power and the produced fusion power to alpha particles is mainly due to ending the simulations when particles still had 100keV of their energy left and, to a lesser extent, numerical inaccuracies in the simulations. The plasma currents of the discharges have been included since they are essential when comparing the power depositions.

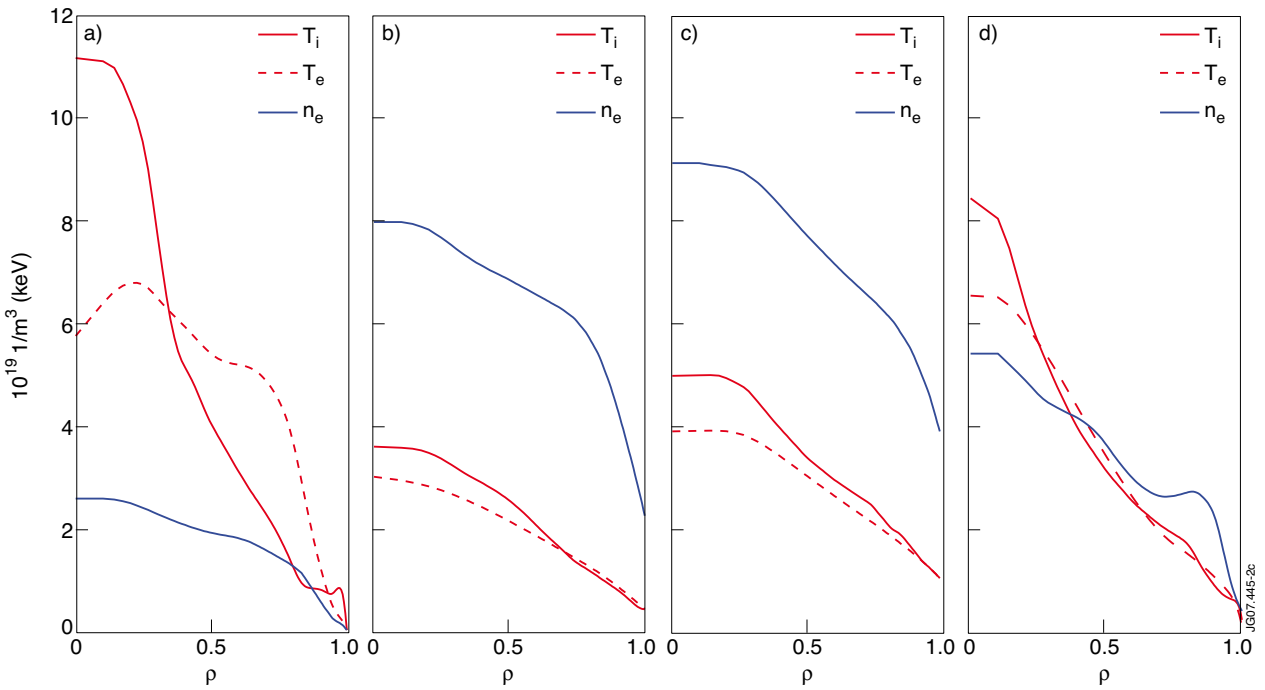

Figure 1: Radial profiles of temperatures and densities as a function of the normalized poloidal flux ρ for the four discharges studied a) #51976 at t = 4.8s, b) #50844 at t = 21.5 s, c) #52009 at t = 21.0s, and d) #66498 at t = 7.1 s. The profiles, the ion temperatures in particular, indicate that a) and d) are advanced scenario discharges with an ITB, whereas b) and c) are ELMy H-mode discharges.

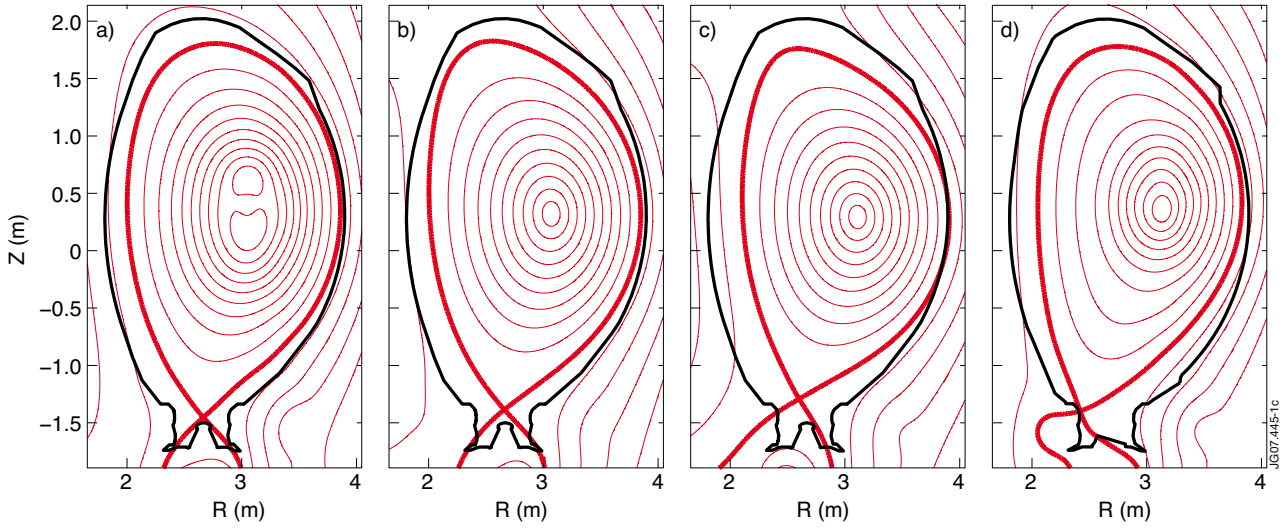

Figure 2: The flux surface structures of the four JET discharges used in this work a) #51976, b) #50844, c) #52009, and d)#66498. The ρ-surfaces have been plotted at intervals of 0.1, starting from the surface ρ = 0:1.

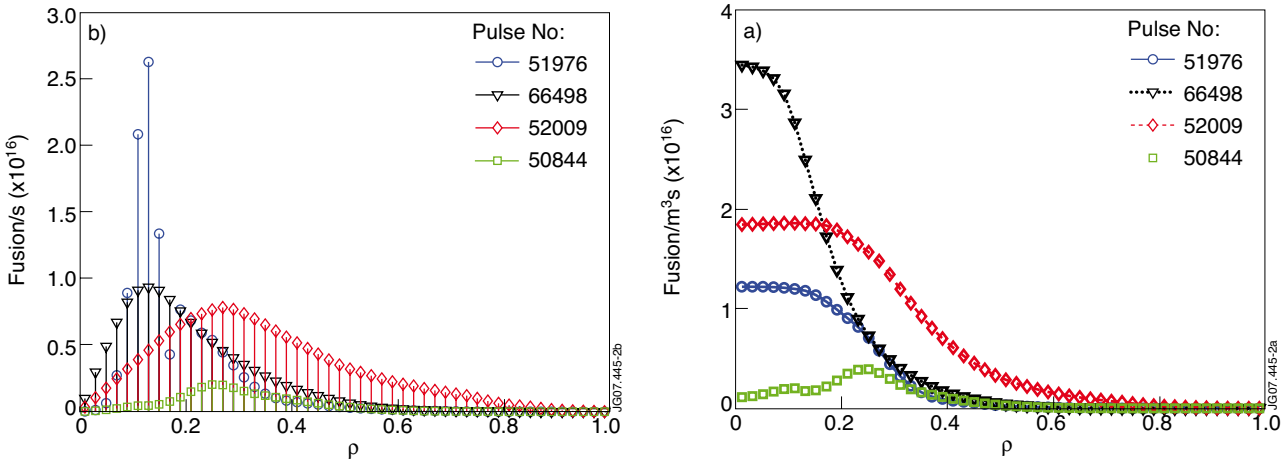

Figure 3: Radial profiles of a) fusion reactivities and b) fusion rates for the four discharges studied in this work. The total fusion reaction rates for the four discharges were: 12.4.10^{16} (#51976), 2.43.10^{16} (#50844), 15.7.10^{16} (#52009), and 7.52¢1016 (#66498) fusions per second.

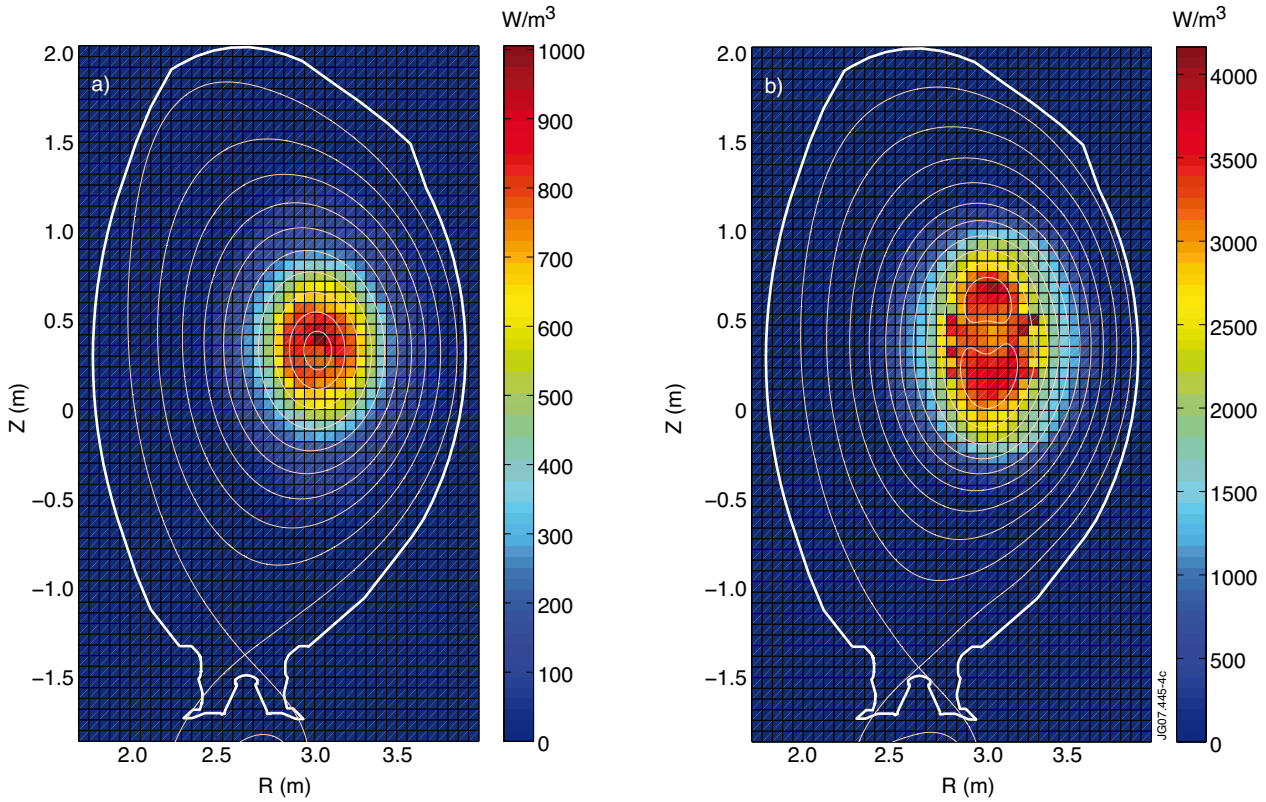

Figure 4: Power deposition patterns of the JET a) H-mode discharge #50844 and b) advanced scenario discharge #51976. The two discharges are comparable due to their identical plasma currents (Ip = 1.9MA) even though their fusion rates, and thus the deposited powers, are very different.

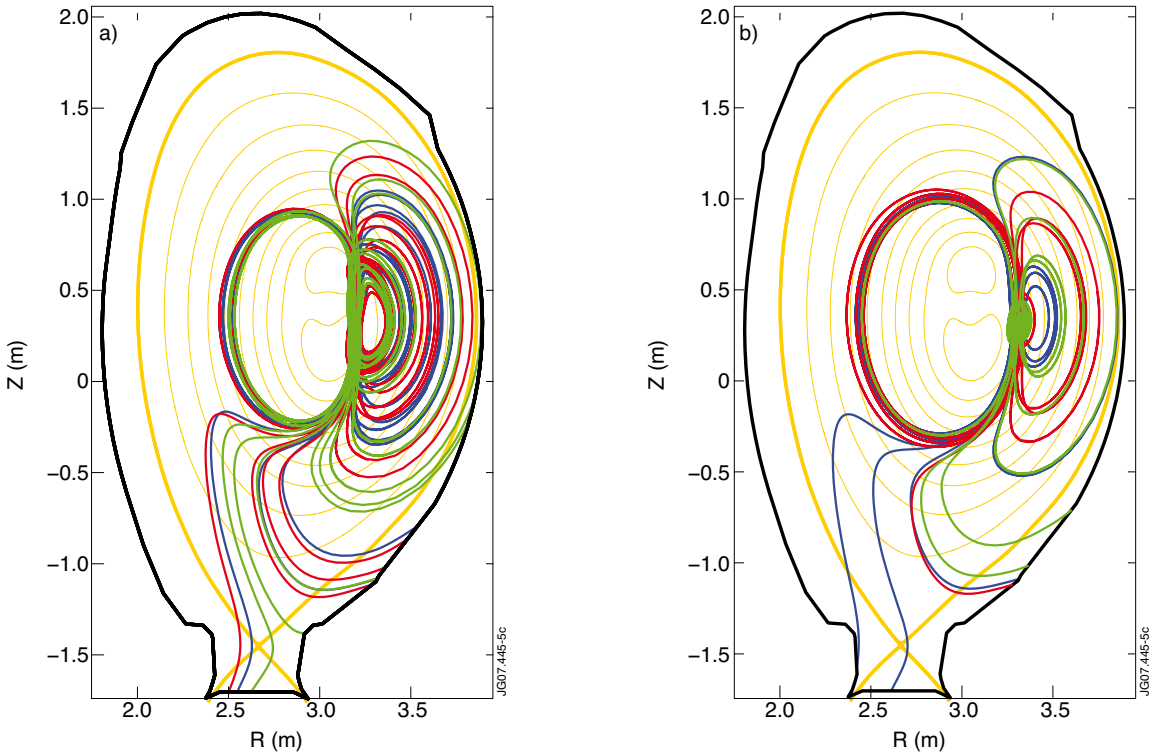

Figure 5: Randomly-chosen particle orbits in discharge #51976. The particles were sent from (a) the region of the plasma with the highest amount of fusions per second, and (b) the approximate stagnation point on the low- field-side of the device.

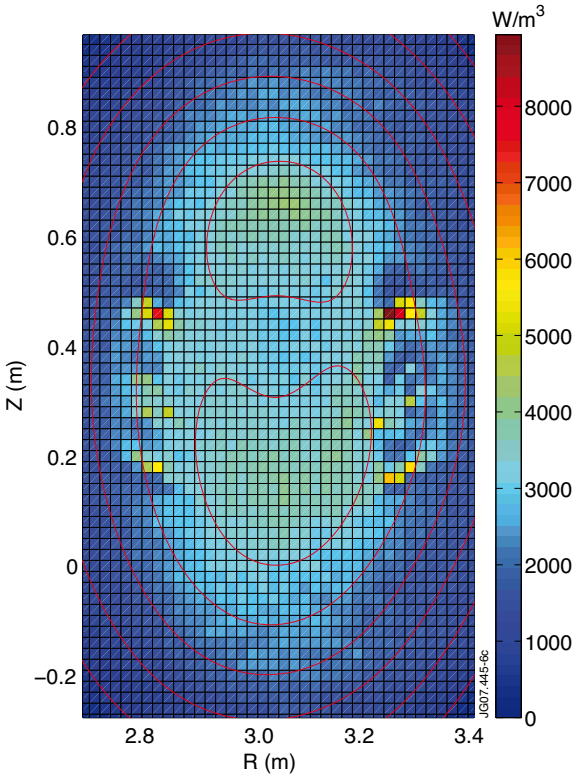

Figure 6: The power deposition pattern in the center of the discharge #51976. The effect of the potato orbits with the stagnation point in the middle is clearly visible both on the high eld and the low field side.